Int. J. Electrochem. Sci., 7 **[2012]** 12633 - 12645

International Journal of
ELECTROCHEMICAL
SCIENCE
www.electrochemsci.org

Effect of Carbon Content on Electrochemical Performance of $LiFePO_4$/C Thin Film Cathodes

Nan Zhou[1,2], Evan Uchaker[2], Yan-Yi Liu[2], Su-Qin Liu[1], You-Nian Liu[1,], and Guo-Zhong Cao[2,*]*

[1] College of Chemistry and Chemical Engineering, Central South University, Changsha, Hunan, 410083, China.
[2] Department of Materials Science and Engineering, University of Washington, Seattle, Washington, 98195, United States.
[*]E-mail: liuyounian@csu.edu.cn; gzcao@u.washington.edu

Received: 26 October 2012 / *Accepted:* 19 November 2012 / *Published:* 1 December 2012

Submicron-sized hydrothermal-grown $LiFePO_4$ particles were added into sucrose-water solution followed with annealing in 600 ℃ for 3 hours in nitrogen to form thin, binder-free and high energy $LiFePO_4$/C composite film cathodes and the effects of carbon content on the microstructure and electrochemical properties of such films were investigated. Carbon from sucrose pyrolysis served as both conducting additive and adhesion binder. The structure characters of the $LiFePO_4$/C films were analyzed by XRD, SEM, BET, *etc.* and the electrochemical properties of the films were studied. It was found that 23wt% carbon content could effectively improve the conductivity of the $LiFePO_4$ material and keep the films intact. The coherent $LiFePO_4$/C composite film cathode is capable of delivering lithium-ion intercalation capacity of 141 mAh g^{-1} and 131 mAh g^{-1} at current density of 85 mA g^{-1} [0.5 C] and 170 mA g^{-1} [1 C], respectively, with a good cyclic stability.

Keywords: Carbon content, $LiFePO_4$, Lithium ion battery, cathode, thin film.

1. INTRODUCTION

The rapid development of our mobile and technology driven society over recent years, has raised strong requirements for thin film lithium ion batteries with reduced dimensions and high power density [1]. With the combination of high theoretical capacity, flat charge/discharge voltage, abundant raw material resources, low cost, and excellent thermal and chemical stability [2, 3], lithium iron phosphate [$LiFePO_4$, denoted as LFP] is considered to be the promising cathodic material for advanced lithium ion batteries [4, 5]. However, the low electrical conductivity of $LiFePO_4$ hinders the wide-spread commercialization as well as the application in high power devices [6-8]. Different synthesis and fabrication methods have been developed and various conducting additives were introduced to improve the electrochemical performance of $LiFePO_4$ thin films [9-12]. For example, silver particles

were first coated on the surface of hydrothermal synthesized $LiFePO_4$ particles to form a $LiFePO_4$-Ag target and then deposited as a film by pulsed laser deposition [11]. Such LFP thin film modified with silver has demonstrated an excellent electrochemical performance and good cyclic stability.

Carbon was confirmed to be an effective additive for the enhancement of electrochemical property of $LiFePO_4$ thin film batteries. $LiFePO_4$ and carbon were co-deposit onto $Si/SiO_2/Ti/Pt$ substrates to form $LiFePO_4$/C thin films through pulsed laser deposition by Lu group [10], conductive carbon here played a central role to improve the Li-ion intercalation properties. Carbon was also applied with precursors before the formation of $LiFePO_4$ thin film as it can act not only as conductive source but also as particle size restrictor and reductive agent to avoid the formation of trivalent iron during synthesis [13, 14]. Uniform and crack-free $LiFePO_4$/C nanocomposite film cathodes were fabricated by spreading $LiFePO_4$/ascorbic acid sol on a Pt coated Si wafer, followed with pyrolysis of ascorbic acid to carbon and crystallize $LiFePO_4$ at elevated temperatures in nitrogen [15]. The resulting $LiFePO_4$/C nanocomposite film demonstrated excellent storage properties partly due to the carbon nanocoating.

More recently $LiFePO_4$/C thin films with high power density were fabricated by drop-casting crystalline $LiFePO_4$ nanoplates colloidal dispersion containing sucrose on titanium foil, followed with pyrolysis at 600℃ for 3hr in nitrogen [16]. The thickness, carbon content, crystallite size, and the porous structure of the $LiFePO_4$/C film cathode could be easily adjusted independently by controlling the hydrothermal growth conditions and casting and pyrolysis process, as well as varying the solid content and sucrose concentration. This film exhibited excellent Li-ion intercalation properties because of the high porosity of the films and fine dispersion of the $LiFePO_4$ nanoplates which guarantees large surface area to ensure fast Faradaic reaction and short transport distance for lithium ion during the intercalation/deintercalation process. In such films, carbon nanocoating serves as both conductive additive as well as binder agent.

For regular carbon coated $LiFePO_4$ cathodes, the thickness of carbon layer was carefully studied [17]. Conclusions were that the conductive performance of LFP could not be effectively improved if the thickness of the carbon layer is too thin; while the intercalation of lithium ions would be retarded by over thicker carbon coating since carbon is considered to be an inert material for Li^+ storage in cathode. For high power $LiFePO_4$ thin films, it is important to investigate the appropriate carbon content, since carbon here not only plays as a conductive promoter but also as an adhesion agent. In this study, micro-sized hydrothermal-grown $LiFePO_4$ particles were added into sucrose-water solution to form thin, binder-free and high energy $LiFePO_4$/C composite film cathodes. The carbon contents in the thin films were adjusted by controlling the concentration of sucrose in the precursor solution. The structure characterization and the electrochemical performance of the films were carefully investigated to optimize the carbon content in the $LiFePO_4$/C composite film cathode.

2. EXPERIMENTAL

2.1 Synthesis of $LiFePO_4$ particles by hydrothermal route

The $LiFePO_4$ powder was prepared via regular hydrothermal route according to the literature [18] by using lithium hydroxide monohydrate $LiOH \cdot H_2O$ [≥ 99.0%, Fluka], Iron[Ⅱ] sulfate

heptahydrate $FeSO_4 \cdot 7H_2O$ [≥ 99.0%, Sigma] and phosphoric acid H_3PO_4 [A.C.S. Reagent, min. 85%, Spectrum] as precursors. In order to reduce Fe^{3+} to Fe^{2+} during the preparation and form a complex with the iron ions [15,18], 1mmol L^{-1} ascorbic acid $C_6H_8O_6$ [≥ 99.0%, Sigma] was added to the 1 mol L^{-1} [content of Fe^{2+}] solution. H_3PO_4 and $FeSO_4 \cdot 7H_2O$ were first dissolved in de-ionized water to form 1 mol L^{-1} solution and then mixed, followed by adding $C_6H_8O_6$. Later, $LiOH \cdot H_2O$ was slowly dropped into the above solution after dissolved in de-ionized water under constant stirring at room temperature. The overall molar ratio of Li:Fe:P was 3:1:1. The obtained mixture was ultrasonicated for 5 minutes and then transferred into a 30ml PTFE lined steel autoclave and heated at 200℃ for 10 hours. After that, the product was cooled to room temperature followed with wash and centrifuge by ethanol and de-ionized water for several times. Pure grayish $LiFePO_4$ powder was obtained after drying in 60℃ overnight.

2.2 Fabrication of the $LiFePO_4$/C films

Four different colloidal dispersions were made by adding 15.8 mg $LiFePO_4$ powder to 5 ml sucrose-water solutions with sucrose content varying from 30 mg, 40 mg, 50 mg, to 60 mg [denoted as S_{30}, S_{40}, S_{50} and S_{60}, respectively]. The suspensions were ultrasonicated for 30 min to make the $LiFePO_4$ particles dispersed homogeneously. The $LiFePO_4$/C composite films were prepared by drop-casting 50 μl of the above suspensions onto Titanium foil wafer and all of them have a geometric area of approximate 0.2 cm^2. The samples were put into small petri dish and covered with edge perforated plastic film. After dried in ambient conditions for 72 hours, all the samples were annealed at 600℃ in N_2 atmosphere for 3 hours.

2.3 Carbon content characterization

To calculate the carbon contents in the four thin films derived from LFP colloidal suspensions with various sucrose mass, films were scratched from Ti substrate and weighted. The obtained powders were added with 0.1 mol/L HCl solution to dissolve $LiFePO_4$. After 30 min ultrasonication, LFP were totally removed and the rest carbon suspension was centrifugated and washed. After drying in 70℃ overnight, the residue carbon powder was weighted and carbon contents were calculated.

2.4 Structural characterization and property measurements

The X-Ray Diffraction [XRD] [D8 Diffractometer] was used to detect the phase of $LiFePO_4$/C composite films. The scanning electron microscopy [SEM] and energy-dispersive X-ray spectroscopy [EDAX] analysis were taken with a JEOL JSM-7000F field emission scanning electron microscope to characterize the morphology and element component of the films. Electrochemical properties of the $LiFePO_4$/C composite films on titanium foils were investigated using a standard three-electrode cell setup. 1 mol l^{-1} $LiClO_4$ in propylene carbonate was used as the electrolyte, Pt foil as the counter electrode and Ag/AgCl as the standard reference electrode, respectively. Cyclic voltammetric [CV]

curves of the $LiFePO_4$/C composite film cathodes were determined using an electrochemical analyzer [CH Instruments, Model 605B]. Galvanostatic charge/discharge cycling performance of the $LiFePO_4$/C composite film cathodes were tested by using a computer controlled electrochemical analyzer [Arbin Instruments, Model BT2000].

3. RESULTS AND DISCUSSION

3.1. Film characterization

Carbon contents in four $LiFePO_4$/C films derived from different sucrose solution were calculated based on the weight measurement. $LiFePO_4$/C thin films with different carbon contents were scratched from the substrate and then weighted. Subsequently the LFP powders were dissolved in 0.1 mol L^{-1} HCl solution, the residual carbon were thoroughly washed, dried, collected, and weighed. The calculated carbon content of four sample films were about 12wt%, 17wt%, 23wt% and 28wt%, respectively.

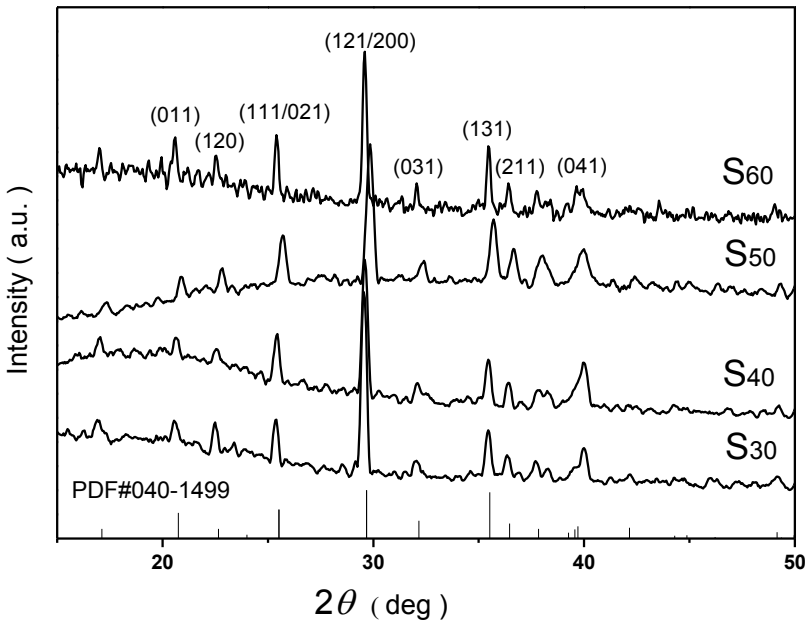

Figure 1. X-Ray Diffraction patterns of $LiFePO_4$/C composite films S_{30}, S_{40}, S_{50} and S_{60} derived from different sucrose solution and LFP- JCPDS standard

Figure 1 summarizes and compares the XRD patterns of four films annealed at 600℃ for 3 hrs in an inert gas, also included in Figure 1 is the standard XRD pattern for $LiFePO_4$. All major peaks in the XRD patterns correspond well with that of typical orthorhombic $LiFePO_4$ [PDF#040-1499], thus indicate the powders obtained from hydrothermal growth were crystalline LFP and the subsequent sucrose treatment had no effect on its crystallinity. No other parasitic phases were detected. Though with relatively high carbon content, no diffraction peaks corresponding to crystalline carbon [graphite]

were found in all XRD patterns, suggesting that the carbon generated from sucrose pyrolysis is likely in the form of amorphous, and its presence has no detectable influence on the crystal structure of $LiFePO_4$.

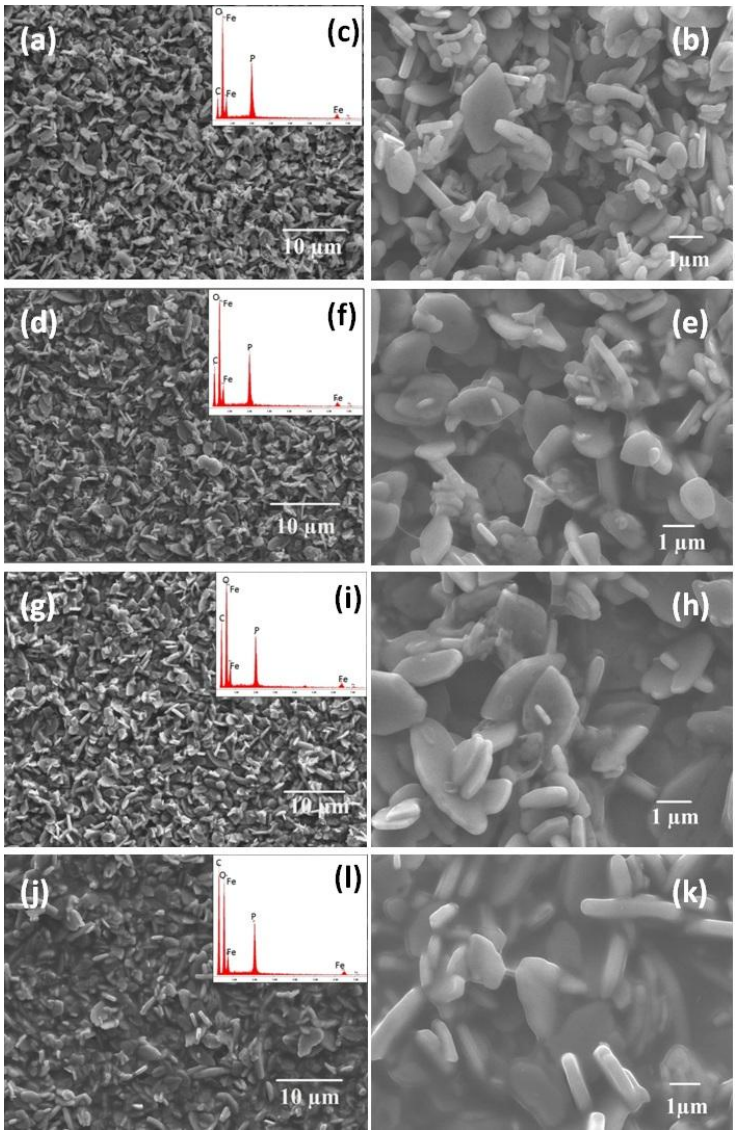

Figure 2. Scanning Electronic Microscopy (SEM) micrographs at low magnification (left) and high magnification (right) and Energy-dispersive X-ray Spectroscopy (EDAX) analysis (insert) of $LiFePO_4$/C composite films derived from different sucrose solution: (a)(b)(c) S_{30}, (d)(e)(f) S_{40}, (g)(h)(i) S_{50} and (j)(k)(l) S_{60}

Figure 2 shows the SEM images with different magnification of four $LiFePO_4$/C composite films derived from $LiFePO_4$/sucrose suspensions with increasing sucrose concentration. The $LiFePO_4$ particles obtained from hydrothermal synthesis have irregular shape, but most of them remained plate-like shape and have an average thickness around 400 nm. As shown in the images, $LiFePO_4$ particles homogeneously dispersed on the titanium substrate while the carbon pyrolyzed from sucrose formed a nice web; together they form a uniform and high porous film. With higher magnification [Figure 2,

right side], the variation in carbon content as a result of different sucrose concentration in the precursor solutions were clearly revealed. For film S_{30} [Figure 2b], prepared from 5ml water solution with 30mg sucrose, amorphous carbon is hard to be detected from the SEM image even with higher magnification; however, with increased sucrose content, films formed from 40mg [Figure 2e] and 50mg [Figure 2h] per 5ml sucrose-water solution show visible carbon webs; when the amount of sucrose in the solution reached 60mg, carbon pyrolyzed from sucrose could form a dense coating of the whole film and almost buried all the $LiFePO_4$ particles, as shown in Figure 2[k]. The elemental composition of four samples were detected by EDAX analysis with the results shown in insert Figure 2[c][f][i] and [l]. The elements detected in all of the patterns corresponding well to $LiFePO_4$, but with a big difference in carbon content for four electrodes. The increasing peaks of carbon found in EDAX patterns with the adding of sucrose verified the carbon residue from sucrose pyrolysis after heat treatment in four sample films, which corroborate qualitatively well with the carbon content determined by dissolving LFP and weighting the remaining carbon. There are some reports that carbon spheres or microbeads are easily obtained from sucrose pyrolysis [19]; however, in the present study, no carbon spheres or beads were detected. The carbon residue was likely to have homogeneously dispersed in the composites and uniformly coated on the surface of $LiFePO_4$ particles.

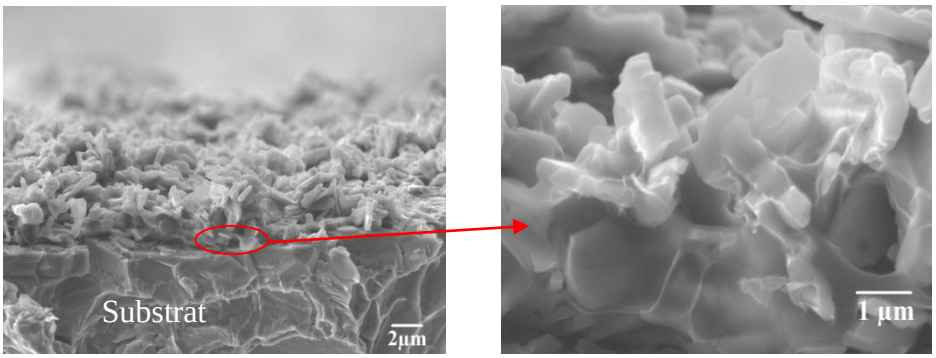

Figure 3. SEM micrographs at low magnification (left) and high magnification (right) for cross-section of sample S_{50}

Figure 3 shows the cross-section of the $LiFePO_4$/C composite film obtained from 50mg per 5ml sucrose-water solution followed with annealing at 600℃ for 3 hours. All the $LiFePO_4$ particles packed irregularly and formed highly porous structure, which permits large interface between the electrolyte and active materials and allows fast intercalation and transfer of Li ions and electrons. The high magnification SEM image also revealed that the carbon derived from sucrose homogeneously dispersed and coated on the surface of $LiFePO_4$ particle. Again, no carbon beads or spheres were found in the film. The well coated carbon on $LiFePO_4$ particles enhanced the transfer of the electrons leading to improved electrochemical properties of LFP raw material. Meantime, the homogeneous carbon dispersion in the film formed a network, which should provide an excellent connection between each $LiFePO_4$ particles, resulting in effective conductive pathways [20].

3.2. Electrochemical properties

$LiFePO_4$/C composite films on titanium foils were assembled directly into a standard three-electrode cell setup to investigate the electrochemical properties, totally get rid of the traditional pre-treatment process and additive adding. 1mol L^{-1} $LiClO_4$ solution in propylene carbonate [PC], Pt foil and Ag/AgCl were used as electrolyte, counter electrode and standard reference electrode respectively. The cyclic voltammetric [CV] curves of four $LiFePO_4$/C composite film cathodes derived from different sucrose content at various scanning rates of 1mV S^{-1}, 2mV S^{-1}, 5mV S^{-1} and 10mV S^{-1} are shown in Figure 4.

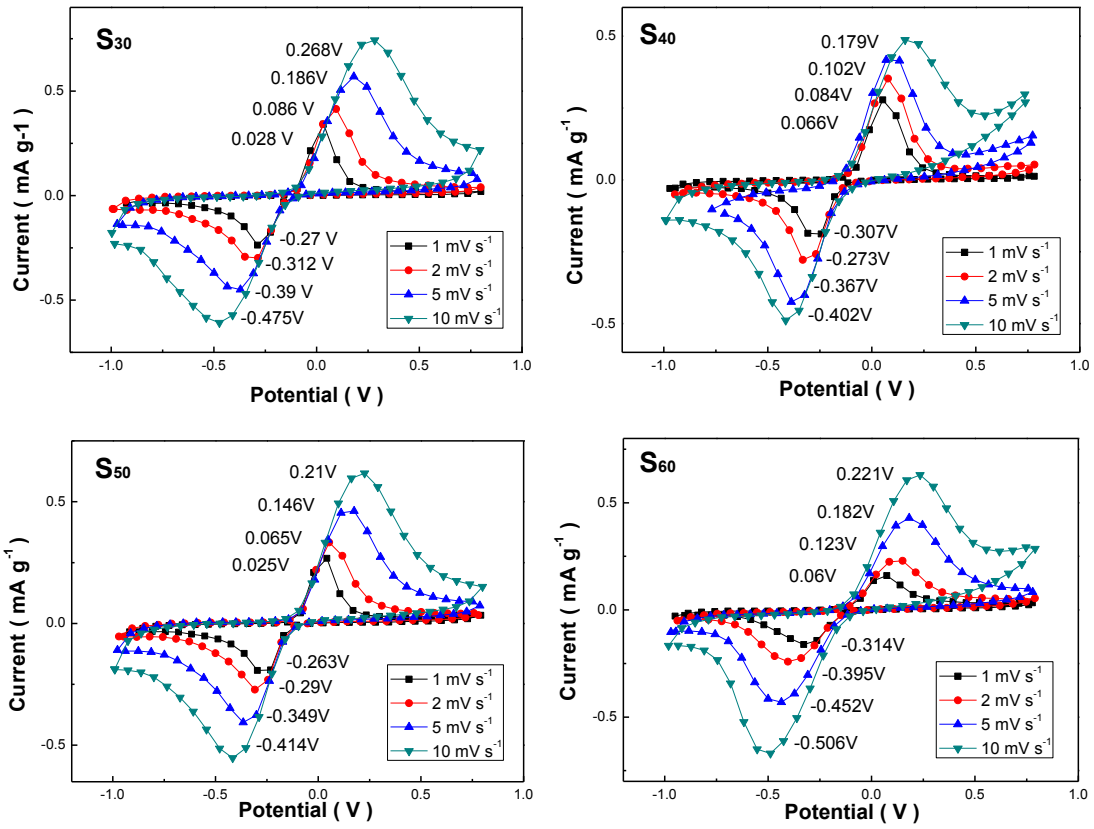

Figure 4. Cyclic voltammetric (CV) curves of $LiFePO_4$/C composite films derived from different sucrose solutions measured at room temperature, at scan rate of 1mV s^{-1}, 2 mV s^{-1}, 5 mV s^{-1} and 10 mV s^{-1}, in a voltage range of -1.4V ~ 1.0V (*vs.* Ag/Ag^+)

Only one couple of cathodic and anodic peaks was found in each CV curve of four samples at various scanning rates. These well defined redox peaks appeared in the range of -0.5V ~ 0.3V [vs. Ag/Ag^+], which should be attributed to the two-phase transformation of Fe^{2+}/Fe^{3+} redox couple, corresponding to lithium ions intercalation/deintercalation of $LiFePO_4$ crystal structure. Even at a high scanning rate of 10mV S^{-1}, the redox peaks of lithium insertion and extraction are distinguishable. Among all the four film cathodes, sharper peaks were found in the CV curves of $LiFePO_4$/C composite film obtained from 50mg $5ml^{-1}$ sucrose-water solution [Figure 4 S_{50}], indicating faster transition of

lithium ions and phase transformation of $LiFePO_4$ crystal structures in this film. The anodic oxidation peak for sample S_{50} appears at 0.025V vs. Ag/Ag^+ and cathodic reduction peak at -0.263V under the scanning rate of 1mV S^{-1}, according to which 0.288V of the hysteresis [ΔV = the difference between the anodic and cathodic peak voltages] can be calculated. However, larger hysteresis of 0.298V, 0.373V and 0.374V were detected for other three films of S_{30}, S_{40} and S_{60}, indicating slower kinetics of these three films when compared with film S_{50}. For a higher scanning rate of 2mV S^{-1}, 5mV S^{-1} and 10mV S^{-1}, all the CV curves show wider gaps between redox peaks; but low hysteresis value could still be obtained for S_{50} $LiFePO_4$/C composite film. There is literature reported that redox reactions would be more effectively when smaller gap between redox peaks of the material was found [21]. It is likely that the $LiFePO_4$/C composite film derived from 50mg $5ml^{-1}$ sucrose-water solution has more desirable microstructure and interface which favor redox reactions and transport processes, leading to better storage performance. This result is in consistent with the galvanostatic charge/discharge cycling results discussed in next paragraphs.

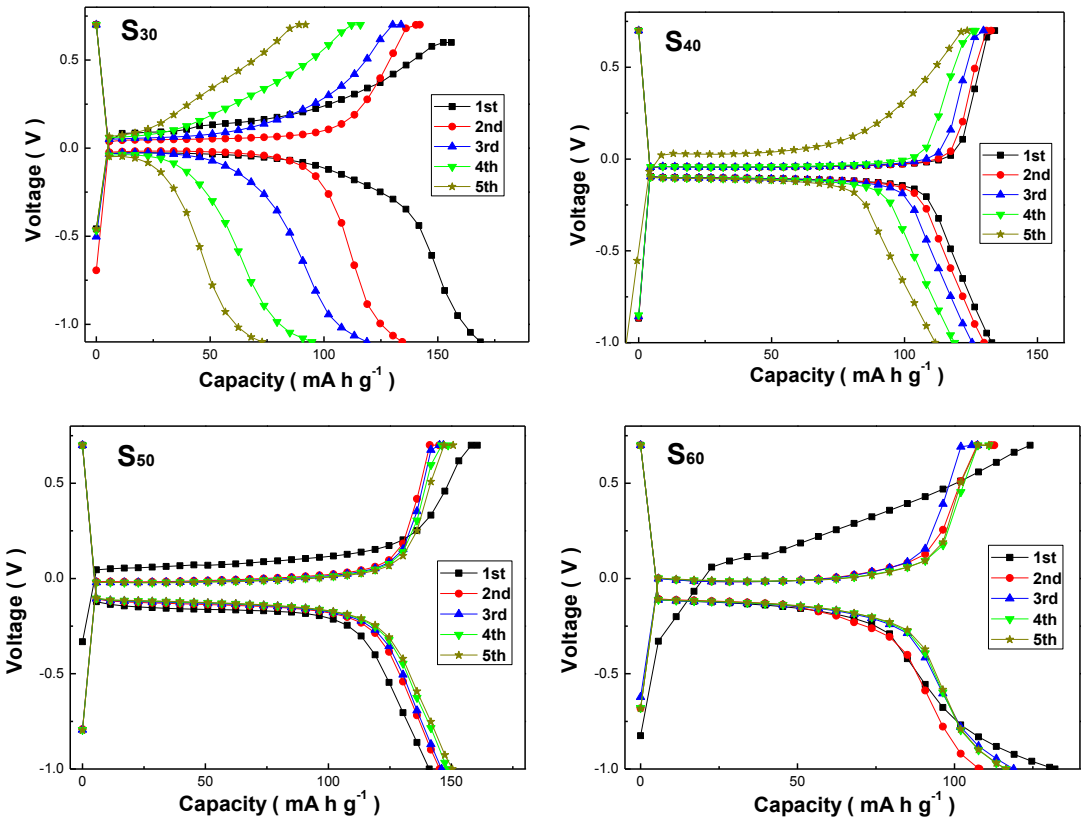

Figure 5. Initial five cycles of charge/discharge performance of $LiFePO_4$/C composite films derived from different sucrose solutions measured at 0.5 C rate, in a voltage range of -1.0V ~ 0.7V (*vs.* Ag/Ag^+)

The storage properties of the $LiFePO_4$/C composite films were analyzed. Only the mass of $LiFePO_4$ was calculated for the specific capacity of the $LiFePO_4$/C composite films. Figure 5 shows the initial five cycles of charge-discharge performance of four samples at 85 mA g^{-1} [0.5 C]. All the

film cathodes exhibited a typical voltage plateau around 0.0V [vs. Ag/Ag^+], which related to the Fe^{2+}/Fe^{3+} redox reactions. Figure 5 show the first five charge/discharge processes of four $LiFePO_4$/C composite thin films with different carbon contents at rate 0.5C. The S_{30} film exhibited a high initial storage capacity of 169 mAh g^{-1}, the same as the theoretical value [170 mAh g^{-1}] of $LiFePO_4$, confirming the fine dispersion of the carbon web effectively improved the conductivity of the whole cathode. However, both the charge and discharge capacities dropped sharply after the first cycle, combined with the shortened plateaus corresponding to the Fe^{2+}/Fe^{3+} two-phase transformation. Only 43% of the initial capacity remained after 5 cycles for this sample. For film S_{40} derived from the solution with 10 more milligram sucrose adding [Figure 5 S_{40}], the fading of the storage capability slowed down when tested at the same condition. The discharge capacity of the 5^{th} cycle still maintained 111.6 mAh g^{-1} while a 132.9 mAh g^{-1} capacity was obtained for the first discharge process. When the sucrose amount in the precursor solution increased to 50 mg, the S_{50} $LiFePO_4$/C film exhibited greatly improved cyclic stability [Figure 5 S_{50}]. The specific capacity value of the S_{50} film at the first cycle turned out to be 141 mAh g^{-1} and then increased gradually. It stabilized at around 150 mAh g^{-1} after five cycles, which is close to the theoretical capacity of $LiFePO_4$. For the fifth cycle, the Columbia efficiency [calculated from discharge capacity/charge capacity] of this film is almost 100% and the irreversible capacity loss between the charge and discharge reaction is only 0.2 mAh g^{-1}. For lithium ion batteries, capacity fading can be contributed to the decomposition of electrolyte, damage of crystal structure, formation of passive film and loss of active material [22-24]. Hydrothermal synthesized $LiFePO_4$ was confirmed to be stable crystal structures and should not be easily damaged during short cycle lives. The electrolyte was also unlikely to be decomposed and form passive films since the charge and discharge capacity of film S_{50} remained well while only the capacity of film S_{30} and S_{40} dropped sharply under the same testing condition. Considering the only difference between four $LiFePO_4$/C composite thin films is the variation of carbon content and carbon here works as a crucial part of adhesion binder, the irreversible capacity loss might be attributed to the missing of active materials, suggesting less carbon content in film S_{30} and S_{40} could not effectively keep the $LiFePO_4$ particles on the Ti substrate stable. This suggestion was further proved by the phenomenon of the capacity fading deceleration of film S_{40} with an increased carbon content of 17wt%, which helped enhancing the adherence of the $LiFePO_4$ particles on the substrate.

The high efficiency and the impressive storage performance exhibited by film S_{50} should be mainly attributed to the suitable carbon content of 23wt%, which formed a uniform coating and webbing connected each $LiFePO_4$ particle to improve the conductivity as well as a strong adhesion stacked the whole LFP material on the substrate to retard capacity fading. Besides, the surface carbon can provide surface defects, which exist as nucleation sites to have phase transition promoted [25, 26]. The lower nucleation activation energy offered by the three-phase interface of $LiFePO_4$-C-electrolyte can also largely accelerate the phase transition during Li-ion intercalation/deintercalation [27-30]. The greatly reduced polarization between the charge and the discharge plateaus in this film after the first charge/discharge process confirms the sluggish penetration of electrolyte through the carbon coating and into the particles' interior, progressively forming an active surface area of $LiFePO_4$ [14]. The two plateaus become steady at 0.0V and -0.25V vs. Ag/Ag^+ after a few cycles respectively, which are in

well agreement with the CV results in Figure 4 S_{50}, suggesting better reversibility than other three films.

However, when the carbon content increased to 28wt%, the lithium intercalation and deintercalation capacities of the $LiFePO_4$/C film dropped and the polarization between the charge and the discharge plateaus broadened [Figure 5 S_{60}]. The S_{60} film exhibited an initial discharge capacitance of about 132 mAh g^{-1} and then dropped to 108 mAh g^{-1} at the next cycle. It finally became steady around 116 mAh g^{-1} after five cycles. Besides, this film presented a high polarization between the intercalation/deintercalation plateaus, whose results corresponding well with the CV curves in Figure 4 S_{60}. It is commonly accepted that carbon coating can improve the conductivity of the LFP raw material and the contact between the electrolyte and the active substance, thus, leading to greater storage performance and excellent cyclic stability [31-33]. On the other hand, it is easily conceivable that an excessive carbon content will reduce the ratio of the active material and the carbon coating web is intrinsically a physical barrier that hinders the diffusion and transition of lithium ion, both of which leading to capacity loss [17]. The widened redox gap of film S_{60} suggests slow kinetics of the lithium ion transition. The electrochemical analysis results confirm that: a] lower content of carbon could not successfully keep the hydrothermal synthesized micro-sized $LiFePO_4$ particles and maintain the whole material on the substrate wafer; b] higher carbon content is over thick for easily penetration and intercalation of Li ions and leading to poor capacitance storage performance. Actually, only appropriate amount carbon residue would effectively enhance the electrochemical performance as well as cyclic property.

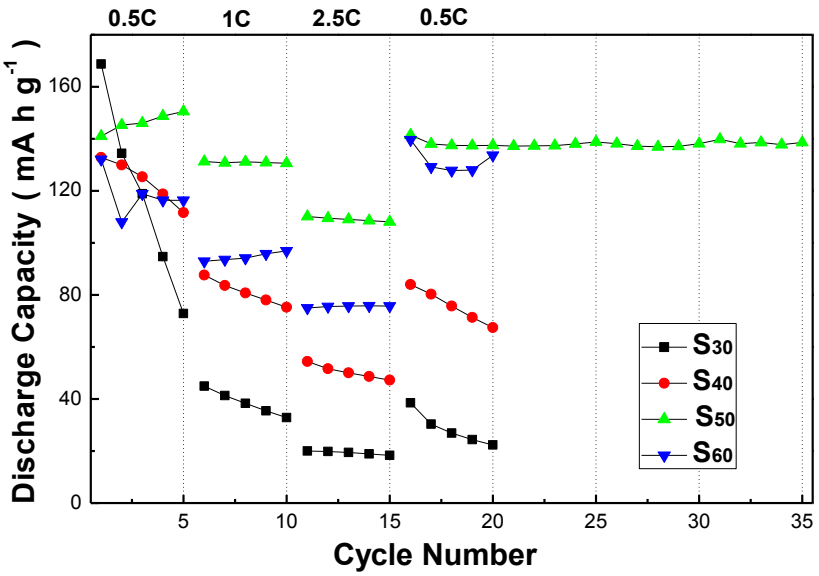

Figure 6. Lithium ion intercalation capacities of $LiFePO_4$/C composite films derived from different sucrose solutions at different discharge rates

Figure 6 shows the lithium intercalation capability of the four $LiFePO_4$/C composite films at different rates of 0.5C, 1.0C, 2.5C and then back to 0.5C. All the samples were cycled 5 times at each

rate and then forwarded to the next step. Although the S_{30} film presented a highest capacitance at the first cycle, it could not hold the lead later. The lithium intercalation capacity of this film dropped sharply to 70 mAh g^{-1} after five cycles and exhibited only 40 mAh g^{-1} and 20 mAh g^{-1} when the discharge current density increased to 0.17 A g^{-1} [1C] and 0.43 A g^{-1} [2.5C] respectively. Even worse is a poor 30 mAh g^{-1} capacity could only be obtained when the discharging rate decreased back to 0.5C. The irreversible capacity fading should attributed mainly to the damage of the whole cathode due to the loss of active materials, which was likely caused by the lack of carbon to bond the loosely packed active material on the Ti substrate during the charge and discharge process. The S_{40} film showed better storage performance of 80 mAh g^{-1} and 50 mAh g^{-1} at 1C and 2.5C, respectively. However, the more than 50% capacity loss after 20 cycles under the same rate test condition demonstrates that the amount of the carbon increase was not enough to stop the $LiFePO_4$/C film cracking and dropping from the substrate. When the sucrose content in the precursor solution adjusted to 50mg, the obtained S_{50} $LiFePO_4$/C film showed an excellent rate performance and impressive cyclic stability. The film exhibited an initial discharge capacity of 141 mAh g^{-1} at 0.5C rate, and remained high capacitance of 130 mAh g^{-1} and 110 mAh g^{-1} when the discharge rate increased to 1C and 2.5C respectively. High lithium storage capacity of 140 mAh g^{-1} was obtained and maintained for more than 35 cycles when the discharge rate dropped back to 0.5C after 16 charging and discharging processes executed at different rates. The excellent storage performance and the good stability should be attributed mainly to the suitable content of carbon, which formed [a] a homogeneous conductive coating on the surface of each $LiFePO_4$ particles; [b] a uniform web connected the whole active material; [c] a strong adhesion to maintain the composite film stable on the Ti substrate during longtime cyclic processes. The excellent storage performance of this S_{50} film indicate that the cathode films fabricated from the $LiFePO_4$ particles in 50mg $5ml^{-1}$ sucrose solution would be well suited for high power lithium ion battery. The film derived from higher sucrose content of 60mg displayed good cyclic stability but frustrating storage properties. The film exhibited only 118 mAh g^{-1}, 95 mAh g^{-1} and 75 mAh g^{-1} at discharge rates of 0.5C, 1C and 2.5C, respectively. The carbon coating from sucrose pyrolysis was over thick and largely hindered the diffusion of lithium ions, resulting in lower intercalation ability, especially at higher discharge current density.

4. CONCLUSIONS

Thin, binder-free and high energy $LiFePO_4$/C composite film cathodes were prepared by adding hydrothermal grown $LiFePO_4$ particles with submicron-size into sucrose-water solution followed with annealing in 600℃ for 3 hours in nitrogen. The contents of carbon in the films could be controlled by adjusting the sucrose amount in the precursor solution. Carbon serves as not only a conducting additive but also an adhesion binder. The surface and microstructure characters have demonstrated that carbon content has appreciable impacts on the electrochemical properties of the $LiFePO_4$/C composite films. This work found that ~23wt% carbon might be needed to ensure the integrity of the composite film and good lithium ion intercalation properties. Lower content of carbon might not be able to retain good adhesion on charge/discharge cycles, while higher content of carbon

would hinder the diffusion of lithium ions resulting in lower storage performance especially in high discharge current density.

ACKNOWLEDGEMENT
NZ gratefully acknowledges the fellowship from China Scholarship Council. This research work has been financially supported in part by the National Science Foundation [NSF, CMMI-1030048], and the University of Washington CGF grant.

References

1. J. L. Li, C. Daniel, D. Wood, *J. Power Sources,* 196 (2011) 2452.
2. A. S. Andersson, J. O. Thomas, B. Kalska, L. Haggstrom, *Electrochem. Solid-State Lett.,* 3 (2000) 66.
3. S. T. Myung, S. Komaba, N. Hirosaki, H. Yashiro, N. Kumagai, *Electrochim. Acta,* 49 (2004) 4213.
4. V. Etacheri, R. Marom, R. Elazari, G. Salitra, D. Aurbach, *Energy Environ. Sci.,* 4 (2011) 3243.
5. J. Wang, X. Sun, *Energy Environ. Sci.,* 5 (2012) 5163.
6. C. Delacourt, L. Laffont, R. Bouchet, C. Wurm, J. B. Leriche, M. Morcrette, J. M. Tarascon, C. Masquelier, *J. Electrochem. Soc.,* 152 (2005) A913.
7. W. Ojczyk, J. Marzec, K. Świerczek, W. Zając, M. Molenda, R. Dziembaj, J. Molenda, *J. Power Sources,* 173 (2007) 700.
8. D. Morgan, A. Van der Ven, G. Ceder, *Electrochem. Solid-State Lett.,* 7 (2004) A30.
9. K. F. Chiu, P. Y. Chen, *Surf. Coat. Technol.,* 203 (2008) 872.
10. Z. G. Lu, M. F. Lo, C. Y. Chung, *J. Phys. Chem. C,* 112 (2008) 7069.
11. Z. Lu, H. Cheng, M. Lo, C. Y. Chung, *Adv. Funct. Mater.,* 17 (2007) 3885.
12. X. J. Zhu, L. B. Cheng, C. G. Wang, Z. P. Guo, P. Zhang, G. D. Du, H. K. Liu, *J. Phys. Chem. C,* 113 (2009) 14518.
13. Y. G. Wang, Y. R. Wang, E. J. Hosono, K. X. Wang, H. S. Zhou, *Angew. Chem. Int. Ed.,* 47 (2008) 7461.
14. X. L. Wu, L. Y. Jiang, F. F. Cao, Y. G. Guo, L. J. Wan, *Adv. Mater.,* 21 (2009) 2710.
15. Y. Liu, D. Liu, Q. Zhang, D. Yu, J. Liu, G. Cao, *Electrochim. Acta,* 56 (2011) 2559.
16. N. Zhou, Y. Liu, J. Li, E. Uchaker, S. Liu, K. Huang, G. Cao, *J. Power Sources,* 213 (2012) 100.
17. Y. D. Cho, G. T. K. Fey, H. M. Kao, *J. Power Sources,* 189 (2009) 256.
18. J. Chen, M. S. Whittingham, *Electrochem. Commun.,* 8 (2006) 855.
19. A. A. Deshmukh, S. D. Mhlanga, N. J. Coville, *Mater. Sci. Eng. R-Rep.,* 70 (2010) 1.
20. J. D. Wilcox, M. M. Doeff, M. Marcinek, R. Kostecki, *J. Electrochem. Soc.,* 154 (2007) A389.
21. J. K. Kim, J. W. Choi, G. S. Chauhan, J. H. Ahn, G. C. Hwang, J. B. Choi, H. J. Ahn, *Electrochim. Acta,* 53 (2008) 8258.
22. P. Arora, R. E. White, M. Doyle, *J. Electrochem. Soc.,* 145 (1998) 3647.
23. P. Ramadass, B. Haran, R. White, B. N. Popov, *J. Power Sources,* 112 (2002) 606.
24. P. Ramadass, B. Haran, R. White, B. N. Popov, *J. Power Sources,* 112 (2002) 614.
25. D. W. Liu, Y. H. Zhang, P. Xiao, B. B. Garcia, Q. F. Zhang, X. Y. Zhou, Y. H. Jeong, G. Z. Cao, *Electrochim. Acta,* 54 (2009) 6816.
26. X. D. Yan, G. Yang, J. Liu, Y. Ge, H. Xie, X. Pan, R. Wang, *Electrochim. Acta,* 54 (2009) 5770.
27. T. Wang, H. Cölfen, M. Antonietti, *J. Am. Chem. Soc.,* 127 (2005) 3246.
28. H. M. Liu, W. S. Yang, Y. Ma, Y. Cao, J. N. Yao, *New J. Chem.,* 26 (2002) 975.
29. M. M. Doeff, J. D. Wilcox, R. Yu, A. Aumentado, M. Marcinek, R. Kostecki, *J. Solid State Electrochem.,* 12 (2008) 995.

30. D. W. Liu, Y. Y. Liu, B. B. Garcia, Q. F. Zhang, A. Q. Pan, Y. H. Jeong, G. Z. Cao, *J. Mater. Chem.*, 19 (2009) 8789.
31. M. M. Doeff, Y. Q. Hu, F. McLarnon, R. Kostecki, *Electrochem. Solid-State Lett.*, 6 (2003) A207.
32. R. Dominko, M. Gaberscek, J. Drofenik, M. Bele, J. Jamnik, *Electrochim. Acta*, 48 (2003) 3709.
33. Z. H. Chen, J. R. Dahn, *J. Electrochem. Soc.*, 149 (2002) A1184